

## ARTICLES

## Detection, measurement, and gravitational radiation

Lee S. Finn

*Department of Physics and Astronomy, Northwestern University, Evanston Illinois 60208*

(Received 20 July 1992)

The optimum design, construction, and use of the Laser Interferometer Gravitational Wave Observatory (LIGO), the French-Italian Gravitational Wave Observatory (VIRGO), or the Laser Gravitational Wave Observatory (LAGOS) gravitational radiation detectors depends upon accurate calculations of their sensitivity to different sources of radiation. Here I examine how to determine the sensitivity of these instruments to sources of gravitational radiation by considering the process by which data are analyzed in a noisy detector. The problem of detection (is a signal present in the output of the detector?) is separated from that of measurement (what are the parameters that characterize the signal in the detector output?). By constructing the probability that the detector output is consistent with the presence of a signal, I show how to quantify the uncertainty that the output contains a signal and is not simply noise. Proceeding further, I construct the probability distribution that the parametrization  $\mu$  that characterizes the signal has a certain value. From the distribution and its mode I determine volumes  $V(P)$  in parameter space such that  $\mu \in V(P)$  with probability  $P$  [owing to the random nature of the detector noise, the volumes  $V(P)$  are always different, even for identical signals in the detector output], thus quantifying the uncertainty in the estimation of the signal parametrization. These techniques are suitable for analyzing the output of a noisy detector. If we are *designing* a detector, or determining the suitability of an existing detector for observing a new source, then we do not have detector output to analyze but are interested in the “most likely” response of the detector to a signal. I exploit the techniques just described to determine the “most likely” volumes  $V(P)$  for detector output that would result in a parameter probability distribution with given mode. Finally, as an example, I apply these techniques to determine the anticipated sensitivity of the LIGO and LAGOS detectors to the gravitational radiation from a perturbed Kerr black hole.

PACS number(s): 04.80.+z, 04.30.+x, 06.20.Dk, 97.60.Lf

## I. INTRODUCTION

Under the present schedule, both the United States Laser Interferometer Gravitational Wave Observatory (LIGO [1, 2]) and the French/Italian VIRGO [3] will begin operation in the late 1990s. Long before that time, theorists must lay a foundation for the study of gravitational radiation sources. Part of this foundation involves the construction of detailed, parametrized models of the wave forms from expected sources; another part involves the calculation of the anticipated sensitivity of the detector to each of these sources. Calculation of these kinds are not only needed for LIGO and VIRGO: design and technology studies for a Laser Gravitational-Wave Observatory in Space (LAGOS) are currently being pursued [4] and calculations of the sensitivity of LAGOS to appropriate sources are needed to guide these studies.

In this paper I address the problem of calculating the anticipated sensitivity of a detector, such as LIGO, VIRGO, or LAGOS, to an arbitrary source of gravitational radiation. The problem breaks up into two parts which I term *detection* and *measurement*. To “detect” is to decide whether the observed detector output contains a signal from a particular source or is just an example of

noise; to “measure” is to assume the presence of a signal in the detector output and to characterize the signal in terms of the parameter(s) that describe the source (and its orientation with respect to the detector).

Echeverria [5] recently examined some of these issues in the particular context of determining the precision with which one could characterize the mass and angular momentum of a perturbed Kerr black hole from observations in a gravitational radiation detector. The foundation of his analysis was the construction of a quantity similar to the signal-to-noise ratio (SNR), and he asserted that the parameters that characterize a signal observed in the output of the detector are those that maximized this quantity. This analysis is limited in two respects [6]: (1) The validity of the formalism is restricted to the limit of high SNR; and (2) the formalism cannot determine the amplitude of the signal. In addition, the conceptual basis of this calculation is not compelling: the determination of the parameters characterizing a signal in a noisy detector does not proceed by maximizing the SNR-like quantity defined by Echeverria [5].

In contrast, the techniques developed here are all based upon the construction of probabilities and probability densities. For the problem of detection, I construct the

probability that the observed detector output is consistent with the presence (or absence) of a signal. In the case of the measurement problem, where the detector output is assumed to include a signal, the quantity constructed is the probability density that describes the likelihood of a given signal parametrization.

In Sec. III, I examine the twin processes of detection and measurement from the point of view of probability theory. The parameters characterizing a signal identified in the output of a noisy detector are defined to be those *most likely* to have resulted in the observed detector output. Some of the results described in this section are known elsewhere in the context of data analysis: they are included here for completeness and so that they may be compared with the techniques employed in Echeverria [5]. In Sec. III, I show how these same techniques can be exploited to evaluate the *anticipated sensitivity* of an instrument to a signal: i.e., how precisely can the parametrization of a signal observed in the detector be determined. I find both exact and, in the interesting limit of a strong signal, approximate techniques for evaluating the expected precision with which an observed signal can be described. As an example, in Sec. IV, I apply the approximate techniques developed in Sec. III to the determination of the parametrization of the gravitational radiation from a perturbed black hole, especially the black hole mass  $M$  and dimensionless angular momentum parameter  $a$ . In Sec. V, I briefly compare the methods and results of Echeverria [5] with my own. My conclusions are presented in Sec. VI.

## II. DETECTION, MEASUREMENT AND PROBABILITY

In this section I consider two related problems that arise in the analysis of the output of a noisy detector: detection and measurement. The problem of detection is to determine whether or not a signal of known form (i.e., deterministic, though parametrized by one or several unknown parameters) is present in the detector output. The problem of measurement is to determine the values of some or all of the unknown parameters that characterize the observed signal.

Note that the distinction between detection and measurement separates the determination of the presence or absence of the signal from the determination of the parameters that characterize it: detection does not address the value of the unknown parameters, and measurement presumes the signal's presence.

Detector noise can always conspire to appear as an example of the sought-for signal; alternatively, noise can mask the presence of a signal. In either case, noise interferes with our ability to determine the presence of the sig-

nal or the parameters that characterize it. Consequently, any claim of detection must be associated with a *probability* signifying the degree of certainty that the detected signal is not, in fact, an instance of noise. Similarly, when an observed signal is characterized it is appropriate to specify both a *range* of parameters and a *probability* that the signal parameters are in the given range.

For example, I can examine the data stream from a gravitational radiation detector to determine (with some probability) whether the radiation from the  $l = |m| = 2$  mode of a perturbed, rotating black hole is present, irrespective of the black hole mass, angular momentum, or orientation with respect to the detector. If I conclude that a signal is present in the data stream, then I can attempt to determine bounds on some or all of these parameters, such that I expect the actual parameters characterizing the signal to fall within those bounds with a given probability.

In the next several subsections I examine detection and measurement in more detail. I assume that the statistical properties of the detector noise are known, and also that the *form* of the sought-for signal is known up to one or several parameters. My discussion focuses on determining the probability that a signal of known form is present in the output of a noisy detector, and on determining the probability that the unknown parameters have particular values.

While the discussion in Sec. IV is framed in the context of the measurement of gravitational radiation from astrophysical sources, the questions addressed in this (and the following) section are purely statistical ones and contain nothing that is specific to gravitational radiation, general relativity, or any particular physical system or theory. For more details, the reader may consult Wainstein and Zubakov [7].

### A. Detection

Consider a data stream  $g(t)$  which represents the output of a detector. The data stream has a noise component  $n(t)$  and in addition may have a signal component  $m(t)$ . The signal component is parametrized by several unknown parameters (denoted collectively as  $\mu$ , and individually as  $\mu_i$ ); hence

$$g(t) = \begin{cases} n(t) & \text{if signal not present,} \\ n(t) + m(t; \mu) & \text{if signal } m(t; \mu) \text{ present.} \end{cases} \quad (2.1)$$

Assume that  $\mu$  is continuous, not discrete. I will describe how to determine the probability that  $m(t; \mu)$ , for *undetermined*  $\mu$ , is present in  $g(t)$ , i.e.,

$$P(m|g) \equiv [\text{the conditional probability that a signal of the form } m(t; \mu), \text{ for unknown } \mu, \text{ is present given the observed data stream } g(t)]. \quad (2.2)$$

Begin by using Baye's law of conditional probabilities to reexpress  $P(m|g)$  as

$$P(m|g) = \frac{P(g|m)P(m)}{P(g)}, \quad (2.3)$$

where

$$P(g|m) \equiv (\text{the probability of measuring } g \text{ assuming the signal } m \text{ is present}), \quad (2.4a)$$

$$P(m) \equiv (\text{the } a \text{ priori probability that the signal } m \text{ is present}), \quad (2.4b)$$

$$P(g) \equiv [\text{the probability that the data stream } g(t) \text{ is observed}]. \quad (2.4c)$$

Also reexpress  $P(g)$  in terms of the two possibilities  $m$  absent and  $m$  present, and further reexpress the probability that  $m$  is present in terms of the probability that it is characterized by the *particular*  $\mu$ :

$$\begin{aligned} P(g) &= P(g|0)P(0) + P(g|m)P(m) \\ &= P(g|0)P(0) + P(m) \int d^N \mu p(\mu) P[g|m(\mu)], \end{aligned} \quad (2.5)$$

where

$$P(0) \equiv (\text{the } a \text{ priori probability that the signal is } \textit{not} \text{ present}), \quad (2.6a)$$

$$P(g|0) \equiv [\text{the probability density of observing } g(t) \text{ in the absence of the signal}], \quad (2.6b)$$

$$P[g|m(\mu)] \equiv [\text{the probability density of observing } g(t) \text{ assuming } m(t; \mu) \text{ with } \textit{particular} \mu \text{ is present}], \quad (2.6c)$$

$$p(\mu) \equiv [\text{the } a \text{ priori probability density that } m(t) \text{ is characterized by } \mu]. \quad (2.6d)$$

Combining Eqs. (2.3) and (2.5), we find

$$P(m|g) = \frac{\Lambda}{\Lambda + P(0)/P(m)}, \quad (2.7)$$

where

$$\Lambda \equiv \int d^N \mu \Lambda(\mu), \quad (2.8)$$

$$\Lambda(\mu) \equiv p(\mu) \frac{P[g|m(\mu)]}{P(g|0)}. \quad (2.9)$$

In Eq. (2.7) all of the dependencies of  $P(m|g)$  on the data stream  $g$  have been gathered into the *likelihood ratio*  $\Lambda$ . Aside from  $\Lambda$ ,  $P(m|g)$  depends only on the ratio of the *a priori* probabilities  $P(0)$  and  $P(m)$ . In turn, the likelihood ratio depends on two components: the *a priori* probability density  $p(m|\mu)$  and the ratio  $P[g|m(\mu)]/P(g|0)$ .

In order to determine  $P(m|g)$  we must *assess* the *a priori* probabilities and *calculate* the likelihood ratio. It is often the case that we know, or can make an educated guess regarding, the *a priori* probabilities. For example, the sources may be Poisson distributed in time [determining  $P(0)$  and  $P(m)$ ], and they may be homogeneously distributed in space [determining  $p(r) \propto r^2$ , where  $r$  is the distance to the source]. At other times our assessment may be more subjective or based on imperfect knowledge, and in this case we can use the observed distribution of  $\mu$  to test the validity of our assessments using the techniques of hypothesis testing (Winkler [8] Sec. 7).

Now turn to the evaluation of  $P[g|m(\mu)]/P(g|0)$ . To determine this ratio, first note that the conditional probability of measuring  $g(t)$  if the particular signal  $m(t; \mu)$  is present is the same as the conditional probability of measuring  $g'(t) = g(t) - m(t; \mu)$ , assuming that the signal  $m(t; \mu)$  is *not present* in  $g'$ :

$$P[g|m(\mu)] = P[g - m(\mu)|0]. \quad (2.10)$$

Consequently, we can focus on the conditional probability of measuring a data stream  $g(t)$  under the assumption

that no signal is present [ $P(g|0)$ ].

In the absence of the signal,  $g(t)$  is simply an instance of  $n(t)$ . Assume that  $n(t)$  is a normal process with zero mean, characterized by the correlation function  $C_n(\tau)$  [or, equivalently, by the one-sided power spectral density (PSD)  $S_n(f)$ ]. In order to compute the ratio  $P[g|m(\mu)]/P(g|0)$ , consider the continuum limit of the case of discretely sampled data  $\{g_i: i = 1, \dots, N\}$ , with the correspondence

$$g_i = g(t_i), \quad (2.11a)$$

$$t_i - t_j = (i - j)\Delta t, \quad (2.11b)$$

$$\Delta t = \frac{T}{N - 1}. \quad (2.11c)$$

The probability that an individual  $g_i$  is a sampling of the random process  $n(t)$  is given by

$$P(g_i|0) = \frac{\exp\left[-\frac{1}{2} \frac{g_i^2}{C_n(0)}\right]}{[2\pi C_n(0)]^{1/2}} \quad (2.12)$$

and the probability that the ordered set  $\{g_i: i = 1, \dots, N\}$  is a sampling of  $n(t)$  is

$$P(g|0) = \frac{\exp\left[-\frac{1}{2} \sum_{j,k=1}^N C_{jk}^{-1} g_j g_k\right]}{[(2\pi)^N \det \|C_{n,ij}\|]^{1/2}}, \quad (2.13)$$

where  $C_{jk}^{-1}$  is defined by

$$\delta_{jk} \equiv \sum_l C_{n,jl} C_{lk}^{-1} \quad (2.14)$$

and

$$C_{n,ij} \equiv C_n[(i - j)\Delta t] \quad (2.15)$$

[Mathews and Walker [9] Sec. 14-6, Wainstein and Zubakov [7], Eq. (31.11)]. Note that the normalization constant in the denominator of Eq. (2.13) is independent of  $g_i$ ; consequently, it does not affect the *ratio*  $P[g|m(\mu)]/P(g|0)$ . Since it is this ratio that we are inter-

ested in, without loss of generality drop the normalization constant from the following.

To evaluate Eq. (2.13) in the continuum limit, first note that

$$\delta(t_j - t_k) = \lim_{\substack{\Delta t \rightarrow 0 \\ T \rightarrow \infty}} \frac{1}{\Delta t} \delta_{jk}. \quad (2.16)$$

Consequently,

$$\begin{aligned} e^{2\pi i f t_k} &= \sum_j e^{2\pi i f t_j} \delta_{jk} \\ &= \lim_{\substack{\Delta t \rightarrow 0 \\ T \rightarrow \infty}} \frac{1}{\Delta t^2} \sum_j \Delta t e^{2\pi i f t_j} \sum_l \Delta t C_n(t_j - t_l) C^{-1}(t_l, t_k) \\ &= \lim_{\substack{\Delta t \rightarrow 0 \\ T \rightarrow \infty}} \frac{1}{\Delta t^2} \int_{-\infty}^{\infty} dt_j e^{2\pi i f t_j} \int_{-\infty}^{\infty} dt_l C_n(t_j - t_l) C^{-1}(t_l, t_k) \\ &= \lim_{\Delta t \rightarrow 0} \frac{1}{\Delta t^2} \int_{-\infty}^{\infty} dt_l e^{2\pi i f t_l} C^{-1}(t_l, t_k) \int_{-\infty}^{\infty} d\tau e^{2\pi i f \tau} C_n(\tau) \end{aligned} \quad (2.17a)$$

$$= \lim_{\Delta t \rightarrow 0} \frac{1}{\Delta t^2} \frac{1}{2} S_n(f) \widetilde{C}^{-1}(f, t_k). \quad (2.17b)$$

To proceed from Eq. (2.17a) to (2.17b), use the Wiener-Khinchine (cf. Kittel [10], Sec. 28) theorem to relate the PSD  $S_n(f)$  to the correlation function  $C_n(\tau)$  and define

$$\widetilde{C}^{-1}(f, t_k) \equiv \int_{-\infty}^{\infty} dt C^{-1}(t, t_k) e^{2\pi i f t}. \quad (2.18)$$

Consequently, as we approach the continuum limit, we have

$$\widetilde{C}^{-1}(f, t_k) = \lim_{\Delta t \rightarrow 0} \Delta t^2 \frac{2e^{2\pi i f t_k}}{S_n(f)}. \quad (2.19)$$

With  $\widetilde{C}^{-1}$  and Parseval's theorem, we can evaluate the continuum limit of the argument of the exponential in Eq. (2.13):

$$\begin{aligned} \lim_{\substack{\Delta t \rightarrow 0 \\ T \rightarrow \infty}} \sum_{j,k=1}^N C_{jk}^{-1} g_j g_k &= \lim_{\substack{\Delta t \rightarrow 0 \\ T \rightarrow \infty}} \frac{1}{\Delta t^2} \sum_{j,k=1}^N \Delta t^2 C^{-1}(t_j, t_k) g(t_j) g(t_k) \\ &= \lim_{\Delta t \rightarrow 0} \frac{1}{\Delta t^2} \int_{-\infty}^{\infty} dt_j dt_k C^{-1}(t_j, t_k) g(t_j) g(t_k) \\ &= \lim_{\Delta t \rightarrow 0} \frac{1}{\Delta t^2} \int_{-\infty}^{\infty} df dt_k \widetilde{C}^{-1}(f, t_k) \widetilde{g}^*(f) g(t_k) \\ &= 2 \int_{-\infty}^{\infty} df \frac{\widetilde{g}^*(f)}{S_n(|f|)} \int_{-\infty}^{\infty} dt_k e^{2\pi i f t_k} g(t_k) \\ &= 2 \int_{-\infty}^{\infty} df \frac{\widetilde{g}(f) \widetilde{g}^*(f)}{S_n(|f|)}. \end{aligned} \quad (2.20)$$

Here and henceforth we will denote the Fourier transform of  $r(t)$  as  $\widetilde{r}(f)$ .

Since the detector output  $g(t)$  is real,  $\widetilde{g}^*(f) = \widetilde{g}(-f)$ . Define the symmetric inner product  $\langle g, h \rangle$

$$\langle g, h \rangle \equiv \int_{-\infty}^{\infty} df \frac{\widetilde{g}(f) \widetilde{h}^*(f)}{S_n(|f|)} \quad (2.21)$$

for real functions  $g$  and  $h$ . In terms of this inner product,

$$\begin{aligned} \Lambda(\boldsymbol{\mu}) &= p(\boldsymbol{\mu}) \frac{P[g|m(\boldsymbol{\mu})]}{P[g|0]} \\ &= p(\boldsymbol{\mu}) \exp [2 \langle g, m(\boldsymbol{\mu}) \rangle - \langle m(\boldsymbol{\mu}), m(\boldsymbol{\mu}) \rangle]. \end{aligned} \quad (2.22)$$

The likelihood ratio  $\Lambda$  is found by substituting Eq. (2.22) into Eq. (2.8).

To summarize, the probability  $P(m|g)$  that a signal of the class  $m(t; \boldsymbol{\mu})$  is present in the output of the detector  $g(t)$  can be expressed in terms of three *a priori* probabilities [ $P(0)$ ,  $P(m)$ , and  $p(\boldsymbol{\mu})$ ] and the ratio of two conditional probabilities [ $P(m|g)/P(0|g)$ ]. The *a priori* probabilities must be assessed, while the ratio of the conditional probabilities can be calculated. Often we know or can make an educated guess regarding the *a priori* probabilities; at other times our assessment is subjective or otherwise based on imperfect knowledge. Finally we establish a threshold for  $P(m|g)$  [or, equivalently, for  $\Lambda$ ,  $\ln \Lambda$ , or some other surrogate of  $P(m|g)$ ], and say that if the  $P(m|g)$  (or its surrogate) exceeds the threshold then we have detected the signal.

I will not discuss detection further, except to say that

the choice of threshold is influenced by our strategy to minimize errors. The two kinds of errors we can make are to claim the presence of a signal when one is in fact not present (a “false alarm”), or to dismiss an observed  $g(t)$  as noise when a signal is present (a “false dismissal”). In order to minimize the probability of a false alarm (conventionally denoted  $\alpha$ ) we want a large threshold, while to minimize the probability of a false dismissal (conventionally denoted  $\beta$ ) we want a small threshold. One obvious strategy for choosing the threshold is to minimize the sum  $\alpha + \beta$ , i.e., to minimize the probability of making

an error. Alternatively, some other combination of  $\alpha$  and  $\beta$  may be minimized, taking into account the relative seriousness of the different kinds of errors. Regardless, it is inadvisable to blindly choose a threshold for  $P(m|g)$  without careful consideration of the false alarm and false dismissal probabilities that arise and their relative severity.

### B. Measurement

Turn now to the question of measurement. From Eqs. (2.3), (2.5), and (2.9) we have

$$p[m(\boldsymbol{\mu})|g] = [\text{the conditional probability that the particular signal } m(t; \boldsymbol{\mu}) \text{ is present in the data stream } g(t)].$$

$$= \frac{\Lambda(\boldsymbol{\mu})}{\Lambda + P(0)/P(m)}. \quad (2.23)$$

This conditional probability density is directly proportional to  $\Lambda(\boldsymbol{\mu})$  and, since the denominator in Eq. (2.23) is independent of  $\boldsymbol{\mu}$ , it is maximized where  $\Lambda(\boldsymbol{\mu})$  is maximized. If we assume that the signal is present, then the probability density that it is characterized by  $\boldsymbol{\mu}$  is

$$p[m(\boldsymbol{\mu})|g, m] = \frac{\Lambda(\boldsymbol{\mu})}{\Lambda}. \quad (2.24)$$

The goal of the measurement process is to determine a volume  $V(P)$  in parameter space such that  $\boldsymbol{\mu} \in V(P)$  with probability  $P$ . This volume is “centered” on the mode of the distribution  $p[m(\boldsymbol{\mu})|g]$  in a way we define later on. The mode of either  $p[m(\boldsymbol{\mu})|g]$  or  $p[m(\boldsymbol{\mu})|g, m]$  is the  $\boldsymbol{\mu}$  that maximizes  $\Lambda(\boldsymbol{\mu})$ . Denote the mode by  $\hat{\boldsymbol{\mu}}$ .<sup>1</sup> While I will occasionally refer to  $\hat{\boldsymbol{\mu}}$  as the “measured” parametrization of the signal, bear in mind that  $\hat{\boldsymbol{\mu}}$  is only the *most likely* parametrization of the observed signal.

If we assume that the global maximum of  $\Lambda(\boldsymbol{\mu})$  is also a local extremum, then  $\hat{\boldsymbol{\mu}}$  satisfies

$$0 = \frac{\partial \Lambda(\boldsymbol{\mu})}{\partial \mu_i}, \quad (2.25)$$

equivalently,  $\hat{\boldsymbol{\mu}}$  maximizes

$$\ln \Lambda(\boldsymbol{\mu}) = \ln p(\boldsymbol{\mu}) + 2 \langle m(\boldsymbol{\mu}), g \rangle - \langle m(\boldsymbol{\mu}), m(\boldsymbol{\mu}) \rangle, \quad (2.26)$$

i.e., it satisfies

$$0 = \frac{\partial \ln p(\hat{\boldsymbol{\mu}})}{\partial \mu_i} + 2 \left\langle \frac{\partial m}{\partial \mu_i}(\hat{\boldsymbol{\mu}}), g - m(\hat{\boldsymbol{\mu}}) \right\rangle. \quad (2.27)$$

This final set of equations is in general nonlinear and may be satisfied by several different  $\boldsymbol{\mu}$ . Some will represent local maxima, while others will correspond to local minima or inflection points; thus, Eq. (2.25) is a necessary but not sufficient condition for  $\hat{\boldsymbol{\mu}}$ .

An important characterization of the strength of the signal in a detector is the signal-to-noise ratio (SNR).

The “actual” SNR depends on the true parametrization of the signal  $\tilde{\boldsymbol{\mu}}$ . We do not have access to  $\tilde{\boldsymbol{\mu}}$ ; however, we *do* know that the most likely value of  $\tilde{\boldsymbol{\mu}}$  is  $\hat{\boldsymbol{\mu}}$ , and we define the SNR in terms of  $\hat{\boldsymbol{\mu}}$ :

$$\rho^2 = 2 \langle m(\hat{\boldsymbol{\mu}}), m(\hat{\boldsymbol{\mu}}) \rangle. \quad (2.28)$$

The factor of 2 arises because the power spectral density  $S_n(f)$  is one sided while  $\tilde{m}(f)$  is two sided. Note that  $\rho^2$  is expressed in terms of the signal power (i.e., it is proportional to the square of the signal amplitude). There is some ambiguity in the literature over whether “SNR” refers to  $\rho$  or  $\rho^2$ . We avoid the ambiguity by referring to either  $\rho$  or  $\rho^2$  wherever the context demands it.

Having found the distribution  $p[m(\boldsymbol{\mu})|g]$  (or  $p[m(\boldsymbol{\mu})|g, m]$ ), we define the boundary of the volumes  $V(P)$  to be its isosurfaces. The probability  $P$  corresponding to the isosurface  $p[m(\boldsymbol{\mu})|g, m] = K^2$  is

$$P = \int_{p[m(\boldsymbol{\mu})|g, m] \geq K^2} d^N \boldsymbol{\mu} p[m(\boldsymbol{\mu})|g]. \quad (2.29)$$

Note that since the distribution  $p[m(\boldsymbol{\mu})|g, m]$  is not generally symmetric,  $\hat{\boldsymbol{\mu}}$  is not necessarily the *mean* of  $\boldsymbol{\mu}$ . Also, if the distribution  $p[m(\boldsymbol{\mu})|g]$  has more than one local maximum then  $V(P)$  need not be simply connected.

To summarize, suppose we have an observation  $g(t)$  which we assume (or conclude) includes a signal  $m(\tilde{\boldsymbol{\mu}})$  (for unknown  $\tilde{\boldsymbol{\mu}}$ ). We construct the probability density  $p[m(\boldsymbol{\mu})|g, m]$  according to Eq. (2.24), and identify isosurfaces of  $p[m(\boldsymbol{\mu})|g, m]$  as the boundary of probability volumes  $V(P)$  according to Eq. (2.29). Finally, we assert that  $\hat{\boldsymbol{\mu}} \in V(P)$  with probability  $P$ .

### III. MEASUREMENT SENSITIVITY

In Sec. II we saw how to decide whether a signal is present or absent from the output of a noisy detector, and, if present, how to determine bounds on the parametrization of the signal. Now I show how to *anticipate* the precision with which a detector can place bounds on the parametrization that characterizes a signal. In particular, consider an observed  $g(t)$  which contains a signal  $m(t; \tilde{\boldsymbol{\mu}})$  for unknown  $\tilde{\boldsymbol{\mu}}$ . We are interested ultimately in the distribution of

<sup>1</sup>While we assume in what follows that the distribution has a single mode, the generalization to a multimodal distribution is trivial.

$$\delta\mu \equiv \tilde{\mu} - \hat{\mu}, \quad (3.1)$$

where  $\hat{\mu}$  is determined by the techniques discussed in Sec. II. There are an infinity of possible  $g(t)$ 's that can

lead to the same  $\hat{\mu}$  [corresponding to different instances of the noise  $n(t)$ ], and for each there is a different probability distribution  $p[m(\mu)|g]$  [cf. Eq. (2.23)] and a different set of probability volumes  $V(P)$ . We will find the probability volumes  $V(P)$  corresponding to

$$p(\tilde{\mu}|\hat{\mu}) = (\text{the conditional probability density that the signal parametrization is } \tilde{\mu}, \text{ assuming that the mode of the distribution } p[m(\mu)|g] \text{ is } \hat{\mu}). \quad (3.2)$$

I show first how to do this exactly, and then show a useful approximation for strong signals.

The mode  $\hat{\mu}$  of the distribution  $p[m(\mu)|g, m]$  satisfies

$$2 \left\langle m(\tilde{\mu}) - m(\hat{\mu}), \frac{\partial m}{\partial \mu_j}(\hat{\mu}) \right\rangle + \frac{\partial \ln p}{\partial \mu_j}(\hat{\mu}) = -2 \left\langle n, \frac{\partial m}{\partial \mu_j}(\hat{\mu}) \right\rangle \quad (3.3)$$

[cf. Eqs. (2.1) and (2.27)]. Since  $n(t)$  is a normal variable with a zero mean, so are each of the  $\langle n, \partial m / \partial \mu_j \rangle$  on the right-hand side of Eq. (3.3). Denote these random variables  $\nu_i$ :

$$\nu_i \equiv 2 \left\langle n, \frac{\partial m}{\partial \mu_i}(\hat{\mu}) \right\rangle. \quad (3.4)$$

The joint distribution of  $\nu_i$  is a multivariate Gaussian and its properties determine, through Eq. (3.3), the properties of the distribution of  $\delta\mu$ . Consequently we can focus

on the joint distribution of  $\nu_i$ .

Since  $\nu_i$  are normal, their distribution is determined completely by the means  $\bar{\nu}_i$ , which vanish, and the quadratic moments

$$\bar{\nu}_i \bar{\nu}_j = 4 \left\langle n, \frac{\partial m}{\partial \mu_i}(\hat{\mu}) \right\rangle \left\langle n, \frac{\partial m}{\partial \mu_j}(\hat{\mu}) \right\rangle. \quad (3.5)$$

To evaluate the average on the right-hand side, we will use the ergodic principle to turn the ensemble average over the random process  $n$  into a time average over a particular instance of  $n$ . Recalling that a time translation affects the Fourier transform of a function by a change in phase,

$$\mathcal{F}[r(t+\tau)] = e^{-2\pi i f \tau} \mathcal{F}[r(t)], \quad (3.6)$$

write

$$\langle n(t+\tau), r(t) \rangle = \int_{-\infty}^{\infty} dt e^{-2\pi i f \tau} \frac{\tilde{n}(f) \tilde{r}^*(f)}{S_n(f)}. \quad (3.7)$$

Consequently,

$$\begin{aligned} \overline{\langle n, r \rangle \langle n, s \rangle} &= \lim_{T \rightarrow \infty} \frac{1}{2T} \int_{-T}^T d\tau \langle n(t+\tau), r \rangle \langle n(t+\tau), s \rangle \\ &= \lim_{T \rightarrow \infty} \frac{1}{2T} \int_{-T}^T d\tau \int_{-\infty}^{\infty} df \frac{\tilde{n}(f) \tilde{r}^*(f)}{S_n(f)} e^{-2\pi i f \tau} \int_{-\infty}^{\infty} df' \frac{\tilde{n}(f') \tilde{s}^*(f')}{S_n(f')} e^{-2\pi i f' \tau} \\ &= \lim_{T \rightarrow \infty} \frac{1}{2T} \int_{-\infty}^{\infty} df \frac{\tilde{n}(f) \tilde{r}^*(f)}{S_n(f)} \int_{-\infty}^{\infty} df' \frac{\tilde{n}(f') \tilde{s}^*(f')}{S_n(f')} \delta(f+f') \\ &= \lim_{T \rightarrow \infty} \frac{1}{2T} \int_{-\infty}^{\infty} df \frac{\tilde{n}(f) \tilde{n}^*(f) \tilde{r}^*(f) \tilde{s}^*(f)}{S_n(f) S_n(f)} \\ &= \frac{1}{2} \int_{-\infty}^{\infty} df \frac{\tilde{r}^*(f) \tilde{s}^*(f)}{S_n(f)} \\ &= \frac{1}{2} \langle r, s \rangle. \end{aligned} \quad (3.8a)$$

$$= \frac{1}{2} \int_{-\infty}^{\infty} df \frac{\tilde{r}^*(f) \tilde{s}^*(f)}{S_n(f)} \quad (3.8b)$$

$$= \frac{1}{2} \langle r, s \rangle. \quad (3.8c)$$

In going from Eq. (3.8a) to Eq. (3.8b), we used the definition of the PSD of the detector noise  $n(t)$ :

$$S_n(f) \equiv \lim_{T \rightarrow \infty} \frac{1}{T} |\tilde{n}(f)|^2 \quad (3.9)$$

(cf. Kittel [10] Sec. 28). With the result in Eq. (3.8c), we have

$$\begin{aligned} \bar{\nu}_i \bar{\nu}_j &= 4 \left\langle n, \frac{\partial m}{\partial \mu_i}(\hat{\mu}) \right\rangle \left\langle n, \frac{\partial m}{\partial \mu_j}(\hat{\mu}) \right\rangle \\ &= 2 \left\langle \frac{\partial m}{\partial \mu_i}(\hat{\mu}), \frac{\partial m}{\partial \mu_j}(\hat{\mu}) \right\rangle \end{aligned} \quad (3.10a)$$

$$\equiv C_{ij}^{-1}. \quad (3.10b)$$

In terms of the  $C_{ij}$  (i.e. the inverse of  $C_{ij}^{-1}$ ), the joint distribution of  $\nu_i$  is given by

$$p(\nu) = \frac{\exp \left[ -\frac{1}{2} \sum_{i,j} C_{ij} \nu_i \nu_j \right]}{\left[ (2\pi)^N \det \|C_{ij}^{-1}\| \right]^{1/2}}. \quad (3.11)$$

This is also the joint distribution of the quantities

$$-2 \left\langle m(\tilde{\boldsymbol{\mu}}) - m(\hat{\boldsymbol{\mu}}), \frac{\partial m}{\partial \mu_j}(\hat{\boldsymbol{\mu}}) \right\rangle - \frac{\partial \ln p}{\partial \mu_j}(\hat{\boldsymbol{\mu}}) \quad (3.12)$$

that appear on the left-hand side of Eq. (3.3); consequently, we expect that for an observation characterized by a given  $\hat{\boldsymbol{\mu}}$  the probability volumes  $V(P)$  are given implicitly by

$$K^2 \geq \sum_{i,j} C_{ij} \left[ 2 \left\langle m(\tilde{\boldsymbol{\mu}}) - m(\hat{\boldsymbol{\mu}}), \frac{\partial m}{\partial \mu_i}(\hat{\boldsymbol{\mu}}) \right\rangle + \frac{\partial \ln p}{\partial \mu_i}(\hat{\boldsymbol{\mu}}) \right] \\ \times \left[ 2 \left\langle m(\tilde{\boldsymbol{\mu}}) - m(\hat{\boldsymbol{\mu}}), \frac{\partial m}{\partial \mu_j}(\hat{\boldsymbol{\mu}}) \right\rangle + \frac{\partial \ln p}{\partial \mu_j}(\hat{\boldsymbol{\mu}}) \right], \quad (3.13)$$

where

$$P = \int_{\sum_{i,j} C_{ij} \nu_i \nu_j \leq K^2} d^N \boldsymbol{\nu} \frac{\exp \left[ -\frac{1}{2} \sum_{i,j} C_{ij} \nu_i \nu_j \right]}{\left[ (2\pi)^N \det \|C_{ij}^{-1}\| \right]^{1/2}}. \quad (3.14)$$

This result is exact as long as the maximum  $\hat{\boldsymbol{\mu}}$  of  $\Lambda(\boldsymbol{\mu})$  is also a local extremum of  $\Lambda(\boldsymbol{\mu})$ .

As the SNR becomes large the distribution  $p(\tilde{\boldsymbol{\mu}}|\hat{\boldsymbol{\mu}})$  becomes sharply peaked about  $\hat{\boldsymbol{\mu}}$  and the determination of the volume  $V(P)$  is greatly simplified. Suppose that  $\rho^2$  is so large that for  $\tilde{\boldsymbol{\mu}} \in V(P)$  for all  $P$  of interest, the difference  $m(\tilde{\boldsymbol{\mu}}) - m(\hat{\boldsymbol{\mu}})$  can be linearized in  $\delta\boldsymbol{\mu}$ . We then obtain, in place of Eq. (3.3)

$$\sum_i \delta\mu_i C_{ij}^{-1} = -2 \left\langle n, \frac{\partial m}{\partial \mu_j}(\hat{\boldsymbol{\mu}}) \right\rangle - \frac{\partial \ln p}{\partial \mu_j}(\hat{\boldsymbol{\mu}}). \quad (3.15)$$

The random variables  $\delta\boldsymbol{\mu}$  are related to the  $\boldsymbol{\nu}$  by a linear transformation,

$$\delta\mu_i = - \sum_j C_{ij} \left[ \nu_j + \frac{\partial \ln p}{\partial \mu_j}(\hat{\boldsymbol{\mu}}) \right], \quad (3.16)$$

consequently,  $\delta\boldsymbol{\mu}$  are normal with means

$$\overline{\delta\mu_i} = - \sum_j C_{ij} \frac{\partial \ln p}{\partial \mu_j}(\hat{\boldsymbol{\mu}}) \quad (3.17)$$

and quadratic moments

$$\overline{(\delta\mu_i - \overline{\delta\mu_i})(\delta\mu_j - \overline{\delta\mu_j})} = C_{ij}. \quad (3.18)$$

The probability distribution  $p(\delta\boldsymbol{\mu}|\hat{\boldsymbol{\mu}})$  is a multivariate Gaussian [cf. Eq. (3.11)]:

$$p(\delta\boldsymbol{\mu}|\hat{\boldsymbol{\mu}}) = \frac{\exp \left[ -\frac{1}{2} \sum_{i,j} C_{ij}^{-1} (\delta\mu_i - \overline{\delta\mu_i})(\delta\mu_j - \overline{\delta\mu_j}) \right]}{\left[ (2\pi)^N \det \|C_{ij}\| \right]^{1/2}}. \quad (3.19)$$

Note that the matrix  $C_{ij}$  now has acquired a physical meaning: in particular, we see that the variances  $\sigma_i^2$  of  $\delta\mu_i$  are

$$\sigma_i^2 \equiv \overline{(\delta\mu_i - \overline{\delta\mu_i})^2} \\ = C_{ii} \quad (3.20)$$

and the correlation coefficients  $r_{ij}$  are given by

$$r_{ij} \equiv \sigma_i^{-1} \sigma_j^{-1} \overline{(\delta\mu_i - \overline{\delta\mu_i})(\delta\mu_j - \overline{\delta\mu_j})} \\ = \frac{C_{ij}}{\sigma_i \sigma_j}. \quad (3.21)$$

In this sense we say that  $C_{ij}$  is the covariance matrix of the random variables  $\delta\boldsymbol{\mu}$ .

In the strong signal approximation, the surfaces bounding the volume  $V(P)$  are ellipsoids defined by the equation

$$\sum_{i,j} (\delta\mu_i - \overline{\delta\mu_i})(\delta\mu_j - \overline{\delta\mu_j}) C_{ij}^{-1} = K^2, \quad (3.22)$$

where the constant  $K^2$  is related to  $P$  by

$$P = \int_{\sum_{i,j} C_{ij}^{-1} x^i x^j \leq K^2} d^N x \frac{\exp \left[ -\frac{1}{2} \sum_{i,j} C_{ij}^{-1} x^i x^j \right]}{\left[ (2\pi)^N \det \|C_{ij}\| \right]^{1/2}}. \quad (3.23)$$

It is often the case that not all of the parameters that characterize the signal are of physical interest. In that case, we may integrate the probability distribution [Eq. (3.11) or (3.19)] over the uninteresting parameters, leaving a distribution describing just the parameters of physical interest.

Finally we come to the question of when the linearization in Eq. (3.15) is a reasonable approximation. Two considerations enter here.

(1) It is important that the probability contours of interest (e.g. 90%) do not involve  $\delta\boldsymbol{\mu}$  so large that the linearization of  $m(\tilde{\boldsymbol{\mu}}) - m(\hat{\boldsymbol{\mu}})$  is a poor approximation.

(2) It is important that the condition number (cf. Golub and Van Loan [11]) of the matrix  $C_{ij}^{-1}$  be sufficiently small that the inverse  $C_{ij}$  is insensitive to this approximation in the neighborhood of  $\hat{\boldsymbol{\mu}}$ .<sup>2</sup> These two conditions will depend on the problem addressed. If the validity of the linearization procedure is doubtful owing to the violation of either or both of these conditions, then we must fall back on Eq. (3.3) and the exact results in Eqs. (3.13) and (3.14).

#### IV. APPLICATION: A PERTURBED BLACK HOLE

In this section, I show how to use the approximate techniques developed in Sec. III to find the precision with

<sup>2</sup>Recall that the relative error in  $\delta\boldsymbol{\mu}$  is the condition number times the relative error in  $C_{ij}^{-1}$ : for a large condition number, small errors in  $C_{ij}^{-1}$  introduced by the linearization approximation can result in large errors in  $\delta\boldsymbol{\mu}$ .

which the mass and angular momentum of a perturbed black hole can be determined through measurement in an interferometric gravitational wave detector. This problem was first considered by Echeverria [5].

Consider a single interferometric gravitational wave detector and a perturbed black hole of mass  $M$  and dimensionless angular momentum parameter  $a$ . Focus attention on a single oscillation mode of the black hole, e.g. the  $l = m = 2$  mode. The strain measured by the detector has the time dependence of an exponentially damped sinusoid characterized by the four parameters  $Q$ ,  $f$ ,  $V$ , and  $T$ :

$$h(t) = \begin{cases} 0 & \text{for } t < 0, \\ V^{-1/3} e^{-\pi f(t-T)/Q} \sin[2\pi f(t-T)] & \text{for } t > 0. \end{cases} \quad (4.1)$$

For convenience, assume that the perturbation begins abruptly at the *starting time*  $T$ . The *frequency*  $f$  depends inversely on the mass of the black hole, and has a weak dependence on its angular momentum: for the  $l = m = 2$  quasinormal oscillation mode,

$$f \simeq \frac{F(a)}{2\pi M}, \quad (4.2a)$$

$$F(a) \equiv 1 - \frac{63}{100}(1-a)^{3/10} \quad (4.2b)$$

is an accurate semiempirical expression for the real part of the quasi-normal-mode frequency [Echeverria [5], Eq. (4.4) and Table II]. The *quality*  $Q$  is the damping time  $\tau$  measured in units of the frequency  $f$ :

$$Q = \pi f \tau. \quad (4.3)$$

For the  $l = m = 2$  oscillation mode of the black hole,  $Q$  depends entirely on  $a$ :

$$Q \simeq Q(a) \equiv 2(1-a)^{-9/20} \quad (4.4)$$

[Echeverria [5], Eq. (4.3) and Table II]. Finally, the *amplitude*  $V^{-1/3}$  of the wave form depends on the distance to the source, the size of the perturbation, and the relative orientation of the detector and the source.

This peculiar parametrization of the amplitude reflects our expectation that perturbed black holes are distributed uniformly throughout space (i.e.  $V \propto r^3$ ) and that all relative orientations of the detector and the black hole source are equally probable. Additionally, it reflects an assumption that perturbations of any allowed amplitude are equally probable; consequently, the *a priori* distribution  $p(V)$  is uniform. Let us also assume that  $p(a)$ ,  $p(f)$ , and  $p(T)$  are uniform and that there is no *a priori* correlation of  $a$ ,  $f$ ,  $V$ , or  $T$ .

An interferometric gravitational wave detector is naturally a broadband receiver, though it can be operated in a narrow-band mode (cf. Vinet, Meers, Man, and Brill-

let [12], Meers [13], and Krolak, Lobo, and Meers [14]). Assume that the detector response function is uniform in the frequency domain over the bandwidth of the gravitational wave; consequently, the signal component in the output of the detector [ $m(t, \mu)$ ] is equal to the wave form  $h(t; Q, f, V, T)$  [cf. Eq. (4.1)]. Assume also that the noise PSD ( $S_n$ ) of the detector is independent of frequency ( $f$ ) in the bandwidth ( $1/\tau$ ) of the signal (I will discuss the validity of this approximation below).

#### A. The signal-to-noise ratio

As a first step toward finding the precision with which  $a$ ,  $M$ ,  $V$ , and  $T$  can be determined, we calculate the SNR  $\rho^2$ . With  $h$  given by Eq. (4.1), evaluate  $\rho^2$  using Eq. (2.28) to obtain

$$\rho^2 = \frac{2Q^3}{\pi f V^{2/3} (1 + 4Q^2) S_n}. \quad (4.5)$$

This expression is valid to better than a percent as long as the signal is observed for a period of time  $\Delta t \gtrsim 2.5\tau$ .

In arriving at Eq. (4.5) we assumed that the noise PSD is constant over the bandwidth of the signal so that  $S_n = S_h(f)$ . The signal bandwidth  $\Delta f$  is approximately

$$\Delta f \simeq \frac{1}{\tau} = \frac{\pi}{2} (1-a)^{9/20} f. \quad (4.6)$$

For small  $a$  the bandwidth is approximately  $f$ , while for large  $a$  the signal is monochromatic. For small  $a$  the approximation that  $S_n$  is constant over the bandwidth of the signal is only a fair approximation for LIGO (cf. Vogt [1], Abramovici *et al.* [2]) or LAGOS (cf. Faller *et al.* [4]); however, it becomes a good approximation for both detectors when  $a \gtrsim 0.9$  (corresponding to  $\Delta f/f \lesssim \frac{1}{2}$ ).

The amplitude  $V$  depends on the detector orientation with respect to the black hole, the amplitude of the perturbation, and the distance between the black hole and the detector. Average  $\rho^2$  over all possible orientations of the detector with respect to the black hole (cf. Thorne [15] Sec. 9.5.3) to obtain

$$\overline{\rho^2} = \frac{16}{5} \frac{Q^2}{F^2 (1 + 4Q^2)} \frac{\epsilon M}{S_n} \left( \frac{M}{r} \right)^2, \quad (4.7)$$

where  $\epsilon M$  is the total energy radiated by the  $l = m = 2$  mode of the black hole perturbation and  $r$  is the distance of the source.

When operated as a broadband detector, the LIGO advanced detectors will be most sensitive to perturbed black holes with  $50 M_\odot \lesssim M \lesssim 100 M_\odot$  where  $S_n \simeq 10^{-48} \text{ Hz}^{-1}$  (cf. Krolak, Lobo, and Meers [14], Dhurandhar, Krolak, and Lobo [16], Vogt *et al.* [1], Abramovici *et al.* [2]). LAGOS will be most sensitive to perturbed black holes in the range  $10^6 M_\odot \lesssim M \lesssim 10^7 M_\odot$ , where  $S_n \simeq 10^{-42} \text{ Hz}^{-1}$  (cf. Faller *et al.* [4]). Consequently

$$\overline{\rho^2}^{1/2} \simeq 5.8G(a) \begin{cases} \left( \frac{\epsilon}{4 \times 10^{-8}} \right)^{1/2} \left( \frac{3 \text{ Mpc}}{r} \right) \left( \frac{M}{50 M_\odot} \right)^{3/2} \left( \frac{10^{-48} \text{ Hz}^{-1}}{S_n} \right)^{1/2} & \text{LIGO,} \\ \left( \frac{\epsilon}{5 \times 10^{-9}} \right)^{1/2} \left( \frac{3 \text{ Gpc}}{r} \right) \left( \frac{M}{10^6 M_\odot} \right)^{3/2} \left( \frac{10^{-42} \text{ Hz}^{-1}}{S_n} \right)^{1/2} & \text{LAGOS,} \end{cases} \quad (4.8)$$

where

$$G(a) \equiv \frac{37}{200} \left[ \frac{17Q^2}{F^2(1+4Q^2)} \right]^{1/2}. \quad (4.9)$$

For frequencies outside of the range 100–200 Hz, the LIGO PSD  $S_n$  scales with frequency: for frequencies greater than approximately 200 Hz (corresponding to  $M \lesssim 50 M_\odot$ ),  $S_n$  scales as  $f^2$  (cf. Thorne [15], Krolak, Lobo, and Meers [14]), and for frequencies less than 100 Hz ( $M \gtrsim 100 M_\odot$ ) it scales as  $f^{-4}$  (cf. Dhurandhar, Krolak, and Lobo [16]). Similarly, for frequencies outside the range  $10^{-3}$ – $10^{-2}$  Hz the LAGOS PSD  $S_n$  scales with frequency: for  $f \gtrsim 10^{-2}$  Hz it scales as  $f^2$ , and for  $f \lesssim 10^{-3}$  Hz it scales as  $f^{-4}$  (cf. Faller *et al.* [4]). Consequently

$$\overline{\rho^2} \propto \begin{cases} M^{-1}, & M \gtrsim 100 M_\odot, \\ M^5, & M \lesssim 50 M_\odot \end{cases} \quad (4.10)$$

for LIGO and

$$\overline{\rho^2} \propto \begin{cases} M^{-1}, & M \gtrsim 10^7 M_\odot, \\ M^5, & M \lesssim 10^6 M_\odot \end{cases} \quad (4.11)$$

for LAGOS.

Little is known about the rate of, or the energy radiated during, black hole formation (cf. Rees [17], Kochanek, Shapiro, and Teukolsky [18]); however, owing to the extreme sensitivity of both the LAGOS and LIGO detectors, it seems a conservative estimate that the formation of a black hole of mass  $10^6 M_\odot \lesssim M \lesssim 10^7 M_\odot$  anywhere in the universe will be detectable by LAGOS,

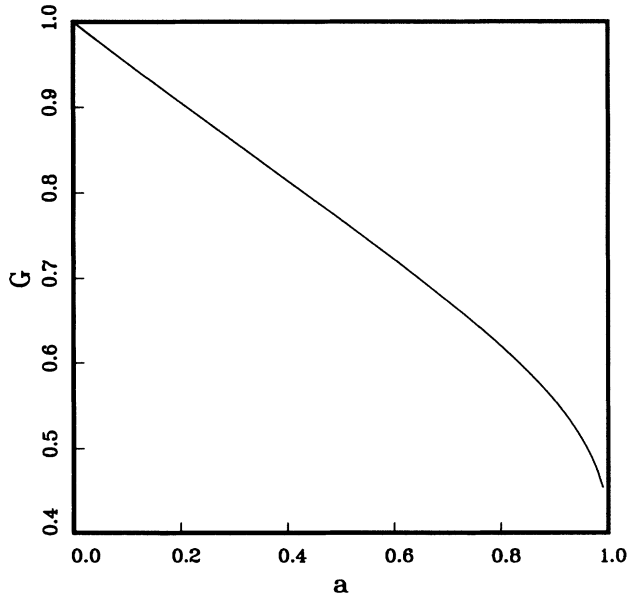


FIG. 1. The expected signal-to-noise ratio (SNR) of the  $l = m = 2$  mode of a perturbed black hole as a function of the angular momentum parameter  $a$ . The dependence of the SNR on the black hole mass, distance, total energy radiated, and the detector noise PSD has been scaled out, leaving only the dependence on the angular momentum parameter. For more details see Eq. (4.8) and the surrounding text.

and the formation of black holes with  $50 M_\odot \lesssim M \lesssim 100 M_\odot$  will be observable in LIGO at least to the distance of the Virgo cluster ( $\sim 10$  Mpc). Additionally, note that the energy radiated in the  $l = 2$  mode during the radial infall of a test body (mass  $m$ ) onto a Schwarzschild black hole (mass  $M$ ) is given by

$$\Delta E = \epsilon M \simeq 10^{-2} \frac{m^2}{M} \quad (4.12)$$

(Davis, Ruffini, Press, and Price [19], Oohara and Nakamura [20]; similar results hold for Kerr black holes: Sasaki and Nakamura [21], Kojima and Nakamura [22]). Consequently, the capture of a solar mass compact object (e.g., a black hole or neutron star) onto a black hole of mass  $10^6$ – $10^7 M_\odot$  (corresponding to  $\epsilon \simeq 10^{-14}$ – $10^{-16}$ ) may also be observable to a distance of 3 Mpc [cf. Eq. (4.8)]

Figure 1 shows the factor  $G(a)$  [cf. Eq. (4.9)] as a function of  $a$ . This figure may also be regarded as a plot of  $\rho(a)$  for fixed  $M$ ,  $\epsilon$ ,  $r$ ,  $S_n$ , and detector-source orientation. With this interpretation, note how  $\rho$  decreases with increasing  $a$ . The reason for this behavior is that at fixed  $M$ , the frequency  $f$  and damping time scale  $\tau$  both increase with  $a$ ; consequently, a signal of smaller amplitude (i.e., smaller  $\rho^2$ ) will yield the same radiated energy.

## B. Precision of measurement

While the parameters  $Q$  and  $f$  are convenient for characterizing the detector response, it is the determination of  $a$  and  $M$  that is of direct physical interest. If the perturbed black hole is also observed electromagnetically (e.g. if it is the result of the gravitational collapse of a star in a type-II supernova), then determination of  $V$  and  $T$  may also be interesting. Regardless, we are more interested in the covariance matrix for the parameters  $\{a, M, V, T\}$  than for the parameters  $\{Q, f, V, T\}$ . It turns out, however, that it is simpler to first determine the covariance matrix for the parametrization  $\{Q, f, V, T\}$ .

To find the covariance matrix for the parametrization  $\{a, M, V, T\}$ , first define the three-dimensionless parameters  $e'$ ,  $\xi'$ , and  $\zeta'$  by

$$\widehat{f}e' \equiv \widetilde{f} - \widehat{f}, \quad (4.13a)$$

$$\widehat{V}\xi' \equiv \widetilde{V} - \widehat{V}, \quad (4.13b)$$

$$\zeta' \equiv \widehat{f}(\widetilde{T} - \widehat{T}), \quad (4.13c)$$

and evaluate  $C_{ij}'^{-1}$  for the parametrization  $\{Q, e', \xi', \zeta'\}$ :

$$2 \begin{pmatrix} \left\langle \frac{\partial h}{\partial Q}, \frac{\partial h}{\partial Q} \right\rangle & \left\langle \frac{\partial h}{\partial Q}, \frac{\partial h}{\partial f} \right\rangle f & \left\langle \frac{\partial h}{\partial Q}, \frac{\partial h}{\partial V} \right\rangle V & \left\langle \frac{\partial h}{\partial Q}, \frac{\partial h}{\partial T} \right\rangle \frac{1}{f} \\ \left\langle \frac{\partial h}{\partial f}, \frac{\partial h}{\partial f} \right\rangle f^2 & \left\langle \frac{\partial h}{\partial f}, \frac{\partial h}{\partial V} \right\rangle fV & \left\langle \frac{\partial h}{\partial f}, \frac{\partial h}{\partial T} \right\rangle \frac{1}{f} \\ \left\langle \frac{\partial h}{\partial V}, \frac{\partial h}{\partial V} \right\rangle V^2 & \left\langle \frac{\partial h}{\partial V}, \frac{\partial h}{\partial T} \right\rangle \frac{V}{f} \\ \left\langle \frac{\partial h}{\partial T}, \frac{\partial h}{\partial T} \right\rangle \frac{1}{f^2} \end{pmatrix}. \quad (4.14)$$

The components of  $C_{ij}'^{-1}$  appearing in Eq. (4.14) are

$$\left\langle \frac{\partial h}{\partial Q}, \frac{\partial h}{\partial Q} \right\rangle = \frac{3 + 6Q^2 + 8Q^4}{2Q^2(1 + 4Q^2)^2} \rho^2, \quad (4.15a)$$

$$\left\langle \frac{\partial h}{\partial Q}, \frac{\partial h}{\partial f} \right\rangle f = -\frac{3 + 4Q^2}{4Q(1 + 4Q^2)} \rho^2, \quad (4.15b)$$

$$\left\langle \frac{\partial h}{\partial Q}, \frac{\partial h}{\partial V} \right\rangle V = -\frac{3 + 4Q^2}{12Q(1 + 4Q^2)} \rho^2, \quad (4.15c)$$

$$\left\langle \frac{\partial h}{\partial Q}, \frac{\partial h}{\partial T} \right\rangle \frac{1}{f} = \frac{\pi \rho^2}{4Q^2}, \quad (4.15d)$$

$$\left\langle \frac{\partial h}{\partial f}, \frac{\partial h}{\partial f} \right\rangle f^2 = \left( \frac{1}{2} + Q^2 \right) \rho^2, \quad (4.15e)$$

$$\left\langle \frac{\partial h}{\partial f}, \frac{\partial h}{\partial V} \right\rangle fV = \frac{\rho^2}{12}, \quad (4.15f)$$

$$\left\langle \frac{\partial h}{\partial f}, \frac{\partial h}{\partial T} \right\rangle = -\frac{\pi \rho^2 (1 + 4Q^2)}{4Q}, \quad (4.15g)$$

$$\left\langle \frac{\partial h}{\partial V}, \frac{\partial h}{\partial V} \right\rangle V^2 = \frac{\rho^2}{18}, \quad (4.15h)$$

$$\left\langle \frac{\partial h}{\partial V}, \frac{\partial h}{\partial T} \right\rangle \frac{V}{f} = 0, \quad (4.15i)$$

$$\left\langle \frac{\partial h}{\partial T}, \frac{\partial h}{\partial T} \right\rangle \frac{1}{f^2} = \frac{\pi^2 \rho^2 (1 + 4Q^2)}{2Q^2}. \quad (4.15j)$$

The components of the covariance matrix  $C'_{ij}$  are

$$C'_{QQ} = \frac{4Q^4 + 3A^2 + 1}{2Q^2 \rho^2}, \quad (4.16a)$$

$$C'_{Qe'} = \frac{1}{2Q^3 \rho^2}, \quad (4.16b)$$

$$C'_{Q\xi'} = \frac{3(4Q^4 + 5Q^2 + 1)}{2Q^3 \rho^2}, \quad (4.16c)$$

$$C'_{Q\zeta'} = -\frac{1}{2\pi \rho^2}, \quad (4.16d)$$

$$C'_{e'e'} = \frac{1 - 2Q^2(1 - 4Q^2)}{2Q^4(1 + 4Q^2)\rho^2}, \quad (4.16e)$$

$$C'_{e'\xi'} = \frac{3(1 - Q^2)}{2Q^4 \rho^2}, \quad (4.16f)$$

$$C'_{e'\zeta'} = -\frac{1}{2\pi \rho^2} \frac{1 - 4Q^2}{Q(1 + 4Q^2)}, \quad (4.16g)$$

$$C'_{\xi'\xi'} = \frac{9(1 + 2Q^2)^2}{2Q^4 \rho^2}, \quad (4.16h)$$

$$C'_{\xi'\zeta'} = -\frac{3}{2\pi Q \rho^2}, \quad (4.16i)$$

$$C'_{\zeta'\zeta'} = \frac{2Q^2}{\pi^2(1 + 4Q^2)\rho^2}. \quad (4.16j)$$

Now define the three-dimensionless parameters  $\epsilon$ ,  $\xi$ , and  $\zeta$  by

$$\widehat{M}\epsilon \equiv \widehat{M} - \widetilde{M}, \quad (4.17a)$$

$$\widehat{V}\xi \equiv \widehat{V} - \widetilde{V}, \quad (4.17b)$$

$$\widehat{M}\zeta \equiv \widehat{T} - \widetilde{T}. \quad (4.17c)$$

The covariance matrix  $C_{ij}$  for the parametrization  $\{a, \epsilon, \xi, \zeta\}$  is given in terms of  $C'_{ij}$  by

$$C_{ij} = \sum_{k,l} \mathcal{J}_{ik}^{-1} C'_{kl} \mathcal{J}_{lj}^{-1}, \quad (4.18)$$

where the symmetric matrix  $\mathcal{J}_{ij}$  is given by

$$\mathcal{J} = \begin{pmatrix} \frac{dQ}{da} - \frac{1}{fM} \frac{df}{da} & 0 & 0 \\ (fM)^2 & 0 & 0 \\ 1 & 0 \\ & & (fM)^2 \end{pmatrix}. \quad (4.19)$$

Like  $C'_{ij}$ , the matrix  $C_{ij}$  is a function only of  $\widehat{a}$  and  $\rho^2$ , and has the elements

$$C_{aa} = \frac{(1 + 2Q^2)(1 + 4Q^2)}{2Q^2 Q'^2} \frac{1}{\rho^2}, \quad (4.20a)$$

$$C_{\epsilon\epsilon} = \left\{ \frac{[QF'(1 + 2Q^2)(1 + 4Q^2) - 2FQ']F'}{2Q^3 Q'^2 F^2} + \frac{1 - 2Q^2 + 8Q^4}{2Q^4(1 + 4Q^2)} \right\} \frac{1}{\rho^2}, \quad (4.20b)$$

$$C_{\xi\xi} = \frac{9(1 + 2Q^2)^2}{2Q^4 \rho^2}, \quad (4.20c)$$

$$C_{\zeta\zeta} = \frac{8Q^2}{(1 + 4Q^2)F^2 \rho^2}, \quad (4.20d)$$

$$C_{a\epsilon} = \frac{Q(1 + 2Q^2)(1 + 4Q^2)F' - FQ'}{2FQ^3 Q'^2 \rho^2}, \quad (4.20e)$$

$$C_{a\xi} = \frac{3(1 + 4Q^2)(1 + Q^2)}{2Q^3 Q'^2 \rho^2}, \quad (4.20f)$$

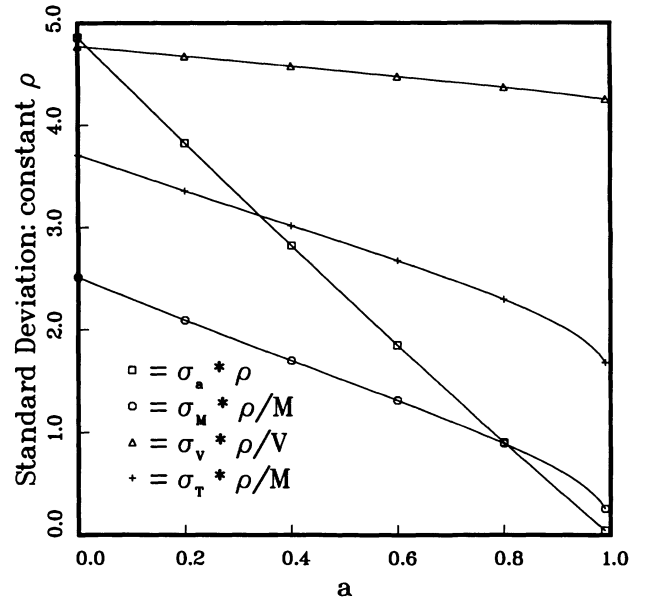


FIG. 2. The expected standard deviation of the black hole angular momentum parameter ( $\sigma_a$ ), mass ( $\sigma_M/M$ ), initial moment of perturbation ( $\sigma_T/M$ ), and perturbation amplitude ( $\sigma_V/V$ ) as a function of the angular momentum parameter  $a$ . The dependence of these standard deviations on the signal-to-noise ratio (SNR)  $\rho$  has been scaled out as shown. For more details see Eqs. (4.20a) and (4.21a)–(4.21c) and the surrounding text.

$$C_{a\zeta} = -(FQ'\rho^2)^{-1} \tag{4.20g}$$

$$C_{\epsilon\xi} = \frac{3 [Q(1+Q^2)(1+4Q^2)F' + (Q^2-1)FQ']}{2Q^4FQ'\rho^2}, \tag{4.20h}$$

$$C_{\epsilon\zeta} = \frac{(1-4Q^2)FQ' - Q(1+4Q^2)F'}{Q(1+4Q^2)F^2Q'\rho^2}, \tag{4.20i}$$

$$C_{\xi\zeta} = -\frac{3}{QF\rho^2}, \tag{4.20j}$$

Eqs. (3.20) and (3.21)]

$$\sigma_M^2 = \widehat{M}^2 \sigma_\epsilon^2, \tag{4.21a}$$

$$\sigma_V^2 = \widehat{V}^2 \sigma_\xi^2, \tag{4.21b}$$

$$\sigma_T^2 = \widehat{T}^2 \sigma_\zeta^2, \tag{4.21c}$$

$$r_{aM} = r_{a\epsilon}, \tag{4.21d}$$

$$r_{aV} = r_{a\xi}, \tag{4.21e}$$

$$r_{aT} = r_{a\zeta}, \tag{4.21f}$$

$$r_{MV} = r_{\epsilon\xi}, \tag{4.21g}$$

$$r_{MT} = r_{\epsilon\zeta}, \tag{4.21h}$$

$$r_{VT} = r_{\xi\zeta}. \tag{4.21i}$$

where  $F(a)$  and  $Q(a)$  are given by Eqs. (4.2b) and (4.4). Finally, in terms of these coefficients, we have (cf.

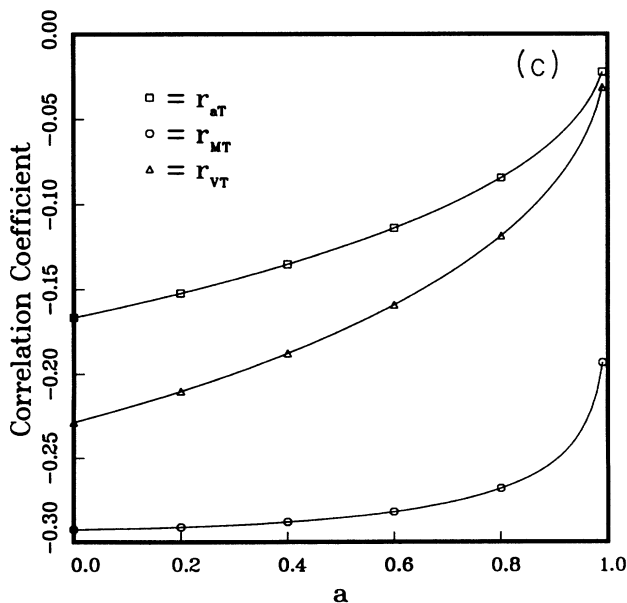
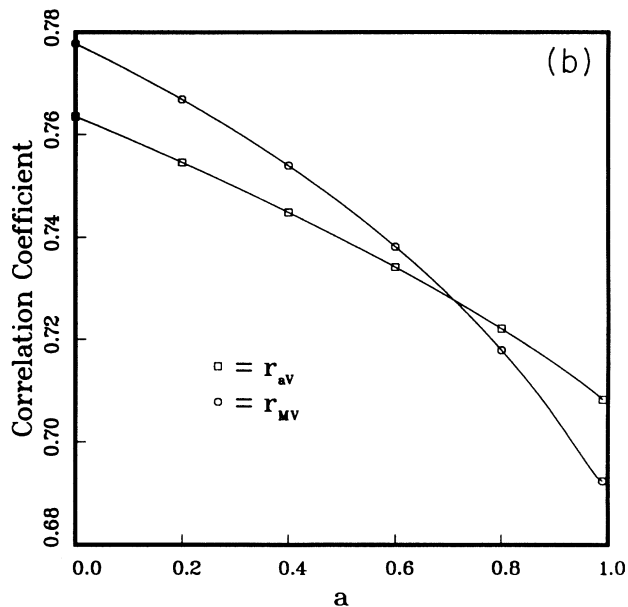
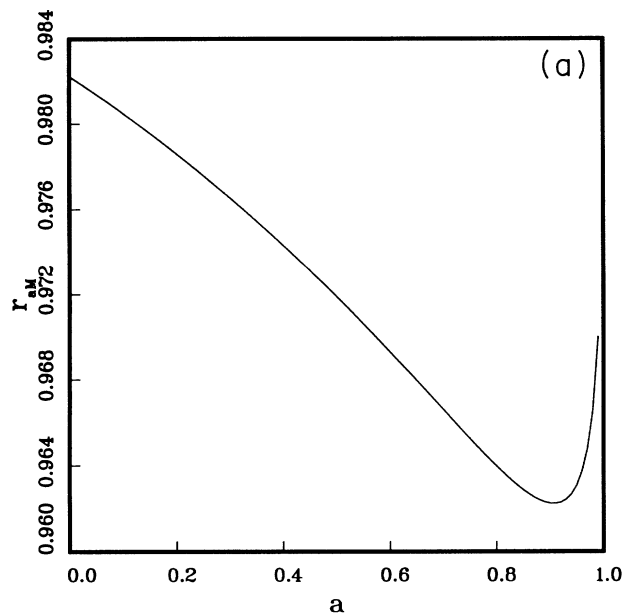


FIG. 3. The correlation coefficients for errors in the angular momentum parameter  $a$ , mass  $M$ , initial moment of perturbation  $T$ , and perturbation amplitude  $V$  as a function of angular momentum parameter. For more details see Eqs. (4.21d)–(4.21i) and the surrounding text.

The results for the standard deviations  $\sigma_a$  and  $\sigma_M/M$  and correlation coefficient  $r_{aM}$  found seminumerically in Echeverria [5] (his Eqs. (4.10a)–(4.10c) and Table II) are approximations to the analytic results found here in Eqs. (4.20a), (4.21a), and (4.21d). Additionally, we give analytic forms of the other variances and correlations coefficients.

Figure 2 shows  $\sigma_a$ ,  $\sigma_M/\widehat{M}$ ,  $\sigma_V/\widehat{V}$ , and  $\sigma_T/\widehat{M}$  [Eqs. (3.20), (4.20a)–(4.20d)], normalized by  $\rho$  as shown, as functions of the measured  $a$ . Note how for  $a \lesssim 0.8$ , the angular momentum parameter is determined less precisely than the mass. Figures 3(a)–3(c) show the six correlation coefficients [cf. Eqs. (3.21) and (4.20e)–(4.20j)] as functions of the measured  $a$ . These are independent of  $\rho$ . In Figs. 3(a)–3(c) note how  $\delta a$  and  $\delta M$  are highly correlated and so are not statistically independent parameters: for a complete discussion of this point, see Echeverria [5] Sec. IV.

Figure 2 shows the standard deviations for fixed  $\rho$ . It is also useful to consider these same quantities for fixed  $M$ ,  $r$ ,  $\epsilon$ , and  $S_n$  as was done in Eq. (4.7) and (4.8) and Fig. 1. Defining  $\rho_0$  by

$$\rho = \rho_0 G(a), \quad (4.22)$$

where  $G(a)$  is given in Eq. (4.9), Fig. 4 shows  $\sigma_a$ ,  $\sigma_M/M$ ,  $\sigma_V/V$ , and  $\sigma_T/M$  normalized by  $\rho_0$  [for LAGOS and LIGO,  $\rho_0$  is given by Eq. (4.8)] and as functions of  $a$ . Note the difference between Figs. 2 and 4: in the first case, the SNR is held constant while in the second the energy of the perturbation is held constant. In the second case, the precision with which  $a$  and  $M$  can be determined does not increase as rapidly with  $a$  as in the first case, the precision with which  $T$  can be determined is independent of  $a$ , and the precision with which the amplitude can be determined *decreases* with increasing  $a$ .

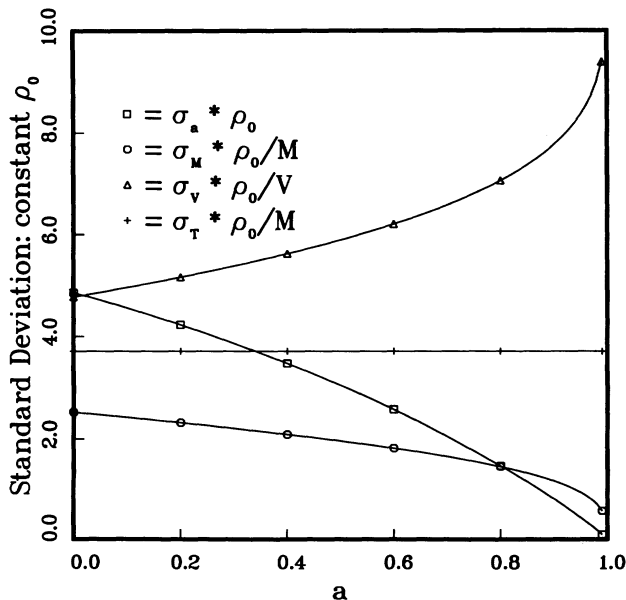


FIG. 4. Like Fig. 2, except that the total energy radiated by the perturbation is held fixed instead of the SNR. Compare with Figs. 1 and 2. For more details see Sec. IV.

The elements of  $C_{ij}^{-1}$  fully determine the distribution  $p[m(\boldsymbol{\mu})|g]$  and the volumes  $V(P)$ . Generally we will have no interest in  $V$  and  $T$ , in which case we integrate the distribution over all  $T$  and  $V$  to find the two-dimensional distribution

$$p[m(a, M)|g] = \frac{\exp \left[ -\frac{1}{2(1-r_{aM}^2)} \left( \frac{\Delta M}{\sigma_M^2} + \frac{\Delta a}{\sigma_a^2} - 2 \frac{\Delta a \Delta M r_{aM}}{\sigma_a \sigma_M} \right) \right]}{2\pi \sigma_a \sigma_M (1-r_{aM}^2)^{1/2}}, \quad (4.23)$$

where

$$\Delta M \equiv M - \widehat{M}, \quad (4.24a)$$

$$\Delta a \equiv a - \widehat{a}. \quad (4.24b)$$

## V. DISCUSSION

The earlier results of Echeverria [5] on the precision of measurement are restricted to the case of large  $\rho$  where the distribution of  $\delta\boldsymbol{\mu}$  is well approximated by a Gaussian, though there is no discussion of what constitutes a sufficiently large SNR. Additionally, those results do not provide any guidance for estimating the precision with which the amplitude of the signal can be measured. Finally, there is no clear connection drawn between the measurement of  $\widehat{\boldsymbol{\mu}}$ , the estimates of  $\overline{\delta\mu_i \delta\mu_j}$ , and the probability that  $|\widehat{\boldsymbol{\mu}} - \boldsymbol{\mu}|^2 \leq \overline{\delta\mu_i^2}$ . The restriction to strong signals is required because of the expansion of Echeverria's [5] expression for  $\rho$  in a power series about the "measured" parameters and also because the methods described fail to take into account prior knowledge about the distribution of the parameters [i.e.,  $p(\boldsymbol{\mu})$ ]. This prior knowledge plays an important role when the distribution of  $\delta\boldsymbol{\mu}$  is not uniform or the SNR is small.

On the other hand, the maximum likelihood analysis described in Sec. II is applicable for all SNR's (though the approximate techniques discussed at the end of Sec. III are appropriate only when the distribution of  $\delta\boldsymbol{\mu}$  is well approximated by a Gaussian). It does not elevate any parameter to a special status: the amplitude of the signal and its precision are determined in the same way that all other signal parameters and their precision are determined. Finally, it gives clear meaning to the measured parameters  $\widehat{\boldsymbol{\mu}}$  and the precision of measurement by providing the probability distribution of the  $\delta\boldsymbol{\mu}$ .

A complete discussion of how the optimal filter techniques of Echeverria [5] are related to the maximum likelihood analysis presented here can be found in Echeverria and Finn [6].

## VI. CONCLUSIONS

In the analysis of the results of an observation made in a detector, it is useful to distinguish between *detection* and *measurement*. The analysis involved in detection refers only to the presence or absence of a signal characterizing a particular *class* of sources to which the detector is sensitive (e.g., perturbed black holes). A particular

source of this class is described by a set of parameters: e.g., among the parameters describing the signal from a perturbed black hole is the black hole mass and angular momentum. Detection addresses only whether a signal of this class is present in the observed output of the detector, and not the particular values of the parameters that best describe the signal.

Measurement follows detection: it refers to the determination of the values of the parameters that best characterize the particular signal *assumed to be present in the detector output* (it only makes sense to speak of measuring the parameters of a real signal). For example, once we have concluded that we have *detected* the signal from the formation of a black hole, then we can go on to *measure* the black hole mass and angular momentum.

In order to determine whether the observed output of a detector includes a signal from a given class of sources, we saw how to calculate the probability that the detector output is consistent with the presence of the signal. That probability depends on the characteristics of the detector noise, the observed detector output, and a parametrized model of the detector response to the signal. In addition, it depends on several *a priori* probabilities that must be assessed. When the calculated probability exceeds a certain threshold then we say that we have detected a signal. Setting the threshold requires careful consideration of the relative severity of falsely claiming a detection and incorrectly rejecting a signal.

To determine the values of the parameters that characterize the detected signal, we saw how to construct the probability distribution that describes how likely different parametrizations  $\mu$  are. We identified  $\hat{\mu}$  as the mode of the distribution, i.e., the parametrization that maximized the probability density, or the *most likely* parametrization. Owing to detector noise,  $\hat{\mu}$  differs in a random fashion from the unknown  $\tilde{\mu}$  that actually describes the signal. We characterized our uncertainty over the actual description of the signal by specifying a volume  $V(P)$  in the parameter phase space, centered on  $\hat{\mu}$ , such that  $\tilde{\mu} \in V(P)$  with probability  $P$ .

We then proceeded to exploit these techniques to *anticipate* the precision with which the parametrization of a particular signal can be determined by a given detector: i.e., we evaluated the *sensitivity* of the detector to

the signal from a class of sources.

To do so, we found the probability distribution of  $\tilde{\mu} - \hat{\mu}$  and defined volumes  $V(P)$  in phase space such that  $\tilde{\mu} \in V(P)$  with probability  $P$ . These volumes determine the precision with which we *expect* we can determine the signal parameters in a real observation. In the interesting limit of a strong signal the anticipated probability distribution of  $\tilde{\mu} - \hat{\mu}$  for fixed  $\hat{\mu}$  is close to Gaussian and the associated volumes  $V(P)$  are ellipsoids. In this limit we found approximate techniques for determining the size and orientation of this ellipsoid. Both the exact and approximate expressions developed provide a powerful means of studying the sensitivity of a proposed detector or detector configuration to a source of gravitational radiation. These techniques are currently being employed to study the sensitivity of the LIGO detectors to binary coalescence [23], precessing axisymmetric neutron stars [24], and nonaxisymmetric neutron stars [25].

As an example of the process of measurement, we evaluated the variance in the mass and angular momentum of a perturbed black hole as determined by observations in a gravitational wave detector. These results improve upon those found earlier (cf. Echeverria [5]), and we discussed the origin of the differences.

The LIGO detector, currently under construction, and the LAGOS detector, currently being designed, are both very sensitive to gravitational radiation from perturbed black holes. A perturbation of a  $50 M_{\odot}$ – $100 M_{\odot}$  black hole that radiates as little as  $10^{-7}$  of the black hole mass should be observable with LIGO at the distance of the Virgo cluster of galaxies, and a perturbation of a  $10^6 M_{\odot}$ – $10^7 M_{\odot}$  black hole that radiates as little as  $10^{-8}$  of the black hole mass should be observable by LAGOS throughout the Universe [cf. Eq. (4.8)].

## ACKNOWLEDGMENTS

I am glad to thank David Chernoff, Fernando Echeverria, Eanna Flanagan, and Kip Thorne for helpful conversations. I also gratefully acknowledge the support of the Alfred P. Sloan Foundation. This work was supported by a grant from the National Aeronautics and Space Administration (NASA Grant No. NAGW-2936).

- 
- [1] R. E. Vogt, "The U.S. LIGO Project," Laser Interferometer Gravitational Wave Observatory Report No. LIGO 91-7, 1991 (unpublished).
  - [2] A. Abramovici, W. E. Althouse, R. W. P. Drever, Y. Gürsel, S. Kawamura, F. J. Raab, D. Shoemaker, L. Sievers, R. E. Spero, K. S. Thorne, R. E. Vogt, R. Weiss, S. E. Whitcomb, and M. E. Zucker, *Science* **256**, 325 (1992).
  - [3] C. Bradaschia *et al.*, *Nucl. Instrum. Methods A* **289**, 518 (1990).
  - [4] J. E. Faller, P. L. Bender, J. L. Hall, D. Hils, R. R. Stebbins, and M. A. Vincent, *Adv. Space Res. (COSPAR)* **9**, 107 (1989).
  - [5] F. Echeverria, *Phys. Rev. D* **40**, 3194 (1989).
  - [6] F. Echeverria and L. S. Finn (unpublished).
  - [7] L. A. Wainstein and L. D. Zubakov, *Extraction of Signals from Noise* (Prentice-Hall, Englewood Cliffs, NJ, 1962).
  - [8] R. L. Winkler, *An Introduction to Bayesian Inference and Decision* (Holt, Rinehart, and Winston., New York, 1972).
  - [9] J. Mathews and R. L. Walker, *Mathematical Methods of Physics* (Benjamin/Cummings, Menlo Park, CA, 1970).
  - [10] C. Kittel, *Elementary Statistical Physics* (Wiley, New York, 1958).
  - [11] G. H. Golub and C. F. Van Loan, *Matrix Computations*, 2nd ed. (Johns Hopkins University Press, Baltimore, 1989).
  - [12] J.-Y. Vinet, B. Meers, C. N. Man, and A. Brilliet, *Phys. Rev. D* **38**, 433 (1988).
  - [13] B. J. Meers, *Phys. Rev. D* **38**, 2317 (1988).
  - [14] A. Krolak, J. A. Lobo, and B. Meers, *Phys. Rev. D* **43**,

- 2470 (1991).
- [15] K. S. Thorne, in *300 Years of Gravitation*, edited by S. W. Hawking and W. Israel (Cambridge University Press, Cambridge, England, 1987), pp. 330–458.
- [16] S. V. Dhurandhar, A. Krolak, and J. A. Lobo, *Mon. Not. R. Astron. Soc.* **237**, 333 (1989).
- [17] M. J. Rees, in *Gravitational Radiation*, edited by N. Deruelle and T. Piran (North-Holland, Amsterdam, 1983), pp. 297–320.
- [18] C. S. Kochanek, S. L. Shapiro, and S. A. Teukolsky, *Astrophys. J.* **320**, 73 (1987).
- [19] M. Davis, R. Ruffini, W. H. Press, and R. H. Price, *Phys. Rev. Lett.* **27**, 1466 (1971).
- [20] K. Oohara and T. Nakamura, *Prog. Theor. Phys.* **70**, 757 (1983).
- [21] M. Sasaki and T. Nakamura, *Prog. Theor. Phys.* **67**, 1788 (1982).
- [22] Y. Kojima and T. Nakamura, *Prog. Theor. Phys.* **71**, 79 (1984).
- [23] L. S. Finn and D. Chernoff (unpublished).
- [24] L. S. Finn (unpublished).
- [25] L. S. Finn (unpublished).